



ELSEVIER

Contents lists available at SciVerse ScienceDirect

Journal of Power Sources

journal homepage: www.elsevier.com/locate/jpowsour



Short communication

A combined photovoltaic and Li ion battery device for continuous energy harvesting and storage

Vidhya Chakrapani*, Florencia Rusli, Michael A. Filler, Paul A. Kohl

School of Chemical & Biomolecular Engineering, Georgia Institute of Technology, Atlanta, GA 30332-0100, USA

HIGHLIGHTS

- Integrated photovoltaic and Li ion battery device for continuous energy harvesting and storage.
- Material and processing challenges involved in building the proposed integrated device.
- Identification of TiN as a diffusion barrier layer for Li ions.

ARTICLE INFO

Article history:

Received 1 April 2012

Received in revised form

15 May 2012

Accepted 18 May 2012

Available online 28 May 2012

Keywords:

Photovoltaic cell

Li ion battery

Integrated device

Silicon nanowires

ABSTRACT

The design, fabrication, and initial analysis of a continuous energy harvesting and storage device for wireless sensor applications were undertaken. A Si nanowire-based photovoltaic (PV) device and Li ion battery were integrated onto a single Si substrate. The three terminal device consisted of separate positive terminals for each component and a shared negative electrode. The effect of Li⁺ incorporation into the planar PV electrode was evaluated. The current–voltage behavior of the PV device was tolerant to high Li⁺ concentrations. A titanium nitride layer between the battery and PV portions of the shared electrode was shown to be an effective diffusion barrier to Li⁺ incorporation.

© 2012 Elsevier B.V. All rights reserved.

1. Introduction

There is a critical need for compact power sources for small, portable electronic devices, such as wireless sensors. Long-lasting power sources can be created by scavenging energy from the environment at low power and storing that energy locally for delivery at high power, as needed by the sensor. The seamless integration of multiple components (i.e. energy harvesting, energy storage, sensing) into a single entity reduces the size and mass of the combined device. One approach is to integrate an efficient energy harvesting system, such as a photovoltaic (PV) cell, with a high density energy storage device, such as a Li ion battery. While nanoscale fuel cells and/or vibration harvesters could also be considered as alternative energy generating devices, their maturity and ease of integration are less established than PV devices.

Prior work on PV-battery modules, such as lead acid technologies combined with PV systems, has used separate components

with interconnected electronics [1]. Such four-electrode devices have a high degree of user control and selection, but require separate packaging of each component which increases the size, mass, and cost of the overall system. The use of a Li ion battery for storage of PV energy is attractive because Li ion devices have high energy density, good charge/discharge efficiency, long lifetime, and robustness under varying load cycles encountered in wireless sensors. Importantly, wireless sensors generally require different power levels for sensing, transmission, and sleep modes.

In this work, several issues dealing with the fabrication and performance of an integrated PV-Li ion battery device built on a single Si substrate with a shared negative electrode were investigated. Fig. 1 shows one configuration of the combined PV-battery device where a nanowire-based Li ion anode is combined with a nanowire-based PV device. However, as is shown in the present work, a planar PV device can also be used with a Si nanowire-based Li ion anode. The latter configuration benefits from the know-how of planar PV technology while retaining a high surface area nanowire Li ion anode. A high surface area battery anode is critical to delivering high current (i.e. power) without a large device footprint.

* Corresponding author. Tel.: +1 2165719977; fax: +1 4048942866.

E-mail address: vchakrapani@gmail.com (V. Chakrapani).

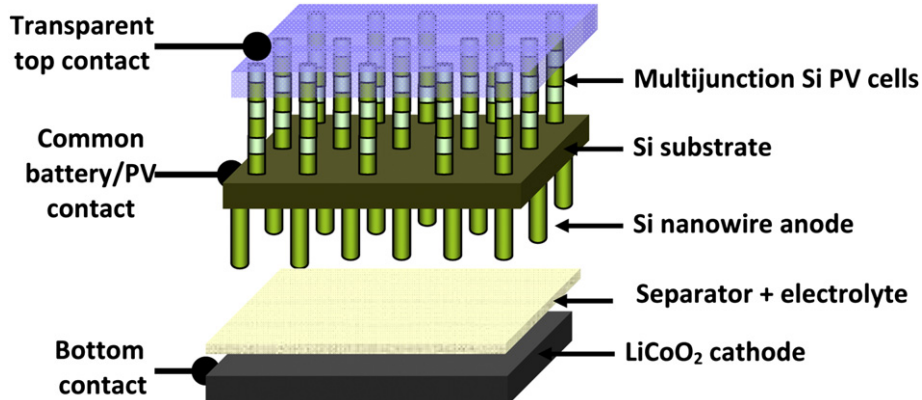


Fig. 1. Schematic illustration of an integrated PV device and Li^+ ion battery module having a common electrode.

The ca. 4 V operation of the Li ion battery can be achieved by use of either a multi-junction PV device or a DC-to-DC energy converter. Charging with a multi-junction PV device via a direct PV-to-battery connection is less desirable than a single junction device with a DC-to-DC converter because a DC-to-DC converter can perform maximum-power tracking in the PV device. The electronic circuitry can also minimize the PV device's dark current, which would have otherwise constituted a self-discharge pathway for the battery. Furthermore, the fabrication of multi-junction PV cells in a planar design would add significant complexity and cost to the PV device.

Si is commonly used as the photoactive layer in PV devices due to its low cost, widespread availability, long-term stability, and well understood material properties. Several techniques have been used to grow Si nanowires including the vapor–liquid–solid (VLS) method. VLS can be used to grow single-crystalline, epitaxial Si nanowires at CMOS-compatible temperatures near 400 °C–500 °C. P-type and n-type doping is readily possible in radial and axial geometries [2,3]. Si PV device efficiencies are currently near 25% and 9% for planar [4] and nanowire [5] architectures, respectively.

The gravimetric capacity of carbon anode in commercial Li ion battery is only $\sim 370 \text{ mAh g}^{-1}$ and may not have the energy or power density to meet the grid-free operation requirements of an integrated wireless sensing module. New, ultrahigh energy density anode materials with longer cycle lifetimes are needed to meet this demand. In this regard, Si-based materials are of interest as the anode for high density Li ion batteries due to their demonstrated lithiation capacity of $\sim 4000 \text{ mAh g}^{-1}$ [6,7]. Unfortunately, structural degradation caused by the large volume expansion of the Si ($>400\%$) during lithiation greatly reduces cycle lifetime. Si nanowires mitigate the mechanical destruction of the silicon through radial strain relaxation. Aligned and random-coiled nanowires have been investigated [6,8]. Despite the advantages of nano-structured electrodes, the volumetric change of the anode during cycling leads to expansion and contraction of the solid–electrolyte-interface (SEI), which causes reconstruction of the layer during deep discharges [9]. Although this consumes electrolyte during deep-discharges, wireless sensors require only intermittent high-power discharge periods for sensing and transmission. Thus, Si nanowire anodes seem well-suited for the high-power, shallow discharge events of wireless sensors.

Since much of the device cost is associated with the substrate, a Si-based, shared electrode module will reduce material cost and could lower the processing costs. In order to integrate a PV and Li ion battery, a number of material and engineering challenges must be overcome. Foremost, Li is a fast diffuser in Si, with a room temperature diffusivity of $2 \times 10^{-10} \text{ cm}^2 \text{ s}^{-1}$ [10]. One of the

primary concerns of the common electrode between the battery and the PV is the back diffusion of Li^+ from the Si battery anode into the PV module, which could degrade the PV device performance. The loss of Li^+ into the bulk substrate will also lower the net battery capacity. The present work examines these material challenges.

2. Experimental

PV devices were fabricated by diffusing B into a n-doped Si (111) wafer (El-Cat, $\rho = 5 \Omega \text{ cm}$). The B doping process was accomplished with an initial predeposition and subsequent drive-in step. During the predeposition step, B was deposited on the device wafer by placing a BN wafer in contact with the Si wafer and heating the pair in a conventional quartz-tube furnace at 1050 °C for 120 min. The drive-in step was performed at 1100 °C for 50 min in a N_2 atmosphere. After drive-in, the samples were cleaned in buffered oxide etch (BOE) to remove the excess boron from the surface. Ohmic contacts to the p-Si regions were made by using sputtered Al metal. The Al contact was annealed in a N_2 atmosphere at 570 °C for 60 min. A sputtered Ti/W film was used for ohmic contacts to the n-Si regions. After metallization, the PV cell was annealed at 450 °C for 60 min in N_2 . Cu leads were attached to the metal contacts using Ag epoxy. No antireflection coating was used. The PV device was covered with insulating epoxy (loctite) except for a small area on the p-doped side used for illumination. The photo-response characteristics of the PV cells were measured at a light intensity of 100 mW cm^{-2} from an AM 1.5 filtered Xenon light source (Newport Instruments).

A TiN diffusion barrier was deposited at room temperature by RF sputtering from a Ti target at 150 W in an 80%Ar/20% N_2 gaseous environment for 100 min. The as-deposited films appeared golden yellow in color. Nominally undoped Si nanowires were grown on top of the TiN film by chemical vapor deposition in a manner similar to that described previously [7,11]. A 5 nm Au film, which served as the catalyst for Si nanowire growth, was deposited on the TiN/W/Ti/Si stack via e-beam evaporation at a pressure less than 10^{-7} Torr. Au droplets were formed upon dewetting and Si nanowires were grown at 550 °C and a total pressure of 15 Torr for 20 min. The partial pressure of SiH_4 and H_2 was 1.4 Torr and 13.6 Torr, respectively. As-grown nanowires were immediately transferred to an Ar filled glove box to minimize exposure to air. The substrate mass was measured before and after growth using a Metler microbalance to determine the mass of Si nanowires.

Electrochemical battery testing was performed in a split, flat cell (MTI Corp.) using metallic Li foil as the counter-reference electrode and Celgard as the separator. No conductive agents or binders were

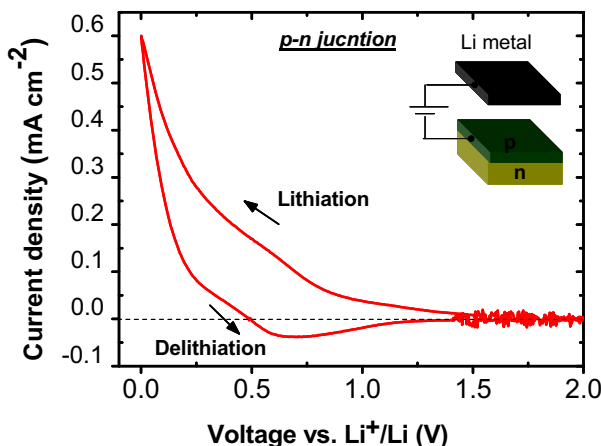


Fig. 2. Cyclic voltammogram of single crystal p–n junction PV device during Li^+ intercalation and deintercalation at a scan rate of 1 mV s^{-1} . The inset in the figure shows the schematics of the electrode arrangement used for electrochemical Li insertion.

used in the electrode fabrication. The electrolyte was 1 M LiPF_6 in a 1:1 mixture of ethylene carbonate (EC) and dimethyl carbonate (DMC). All chemicals were purchased from Sigma–Aldrich. Both electrochemical and PV measurements were performed in an Ar filled glove box, whose H_2O concentration was maintained below 0.1 ppm.

Si nanowire morphology was examined with a Zeiss Ultra60 field emission scanning electron microscope (SEM). Secondary ion mass spectroscopy (SIMS) was used to measure the B and Li dopant concentration in the devices.

3. Results and discussion

The impact of Li^+ diffusion from the battery anode into the PV module is an important consideration in an integrated device. Li^+ is a fast diffuser in Si [10]. The ability of Li^+ to intercalate into many metals and semiconductors is enabled by its small atomic radius relative to the atoms in the host lattice. In fact, there are few known materials that are good diffusion barriers for Li.

In order to evaluate the feasibility of using an integrated device, the effect of Li^+ diffusion on the performance of the PV cell was examined. A single crystal, p–n junction Si PV device was fabricated as described above. Li^+ was subsequently inserted into the device through the p-doped side of the PV device by electrochemical cycling in a LiPF_6 electrolyte. As illustrated in the inset of Fig. 2, the PV device served as the anode and Li metal foil as the counter electrode. Fig. 2 shows a cyclic voltammogram of a PV device measured at a scan rate of 1 mV s^{-1} . The rapid increase in the cathodic current at potentials negative of 0.35 V confirms Li^+ insertion and progressive formation of various Li_xSi alloys [12]. However, very little anodic current was seen during delithiation. This likely resulted from the rapid diffusion of Li^+ deep into the bulk substrate, which makes it unavailable at the surface for subsequent electrochemical reaction in the time frame of the scan rates used here. After the first electrochemical cycle, all subsequent lithiation runs were completed via galvanostatic charging at $180 \mu\text{A cm}^{-2}$ for various times.

Secondary ion mass spectrometry (SIMS) measurements were performed on a lithiated PV device sample to verify Li penetration across the p–n junction. The concentrations of the B and Li in the Si were estimated from the intensity of the secondary ion peaks by comparing the signals to an ion-implanted standard. Fig. 3 shows the B and Li depth profile in the device after electrochemical

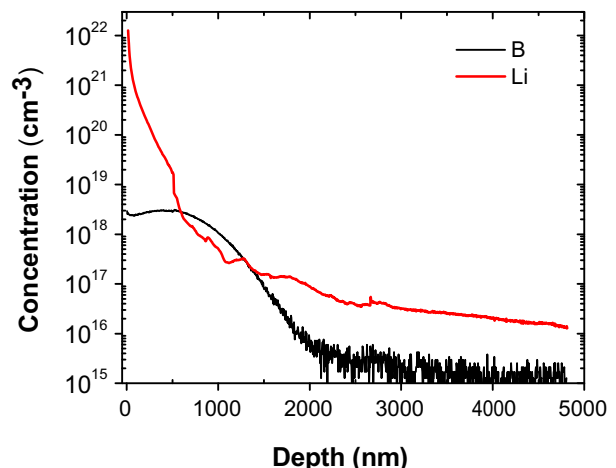


Fig. 3. SIMS depth profile of the boron and Li concentration in a single crystal Si PV device after electrochemical insertion of Li^+ at 0.57 C cm^{-2} .

charging at 0.57 C cm^{-2} . Based on the B concentration profile and initial concentration of P in the substrate, the p–n junction depth was estimated to be $1.7 \mu\text{m}$ from the surface. The Li concentration profile is consistent with our galvanostatic cycling data; exhibiting a large concentration near the surface and a tail extending several micrometers into the substrate.

The current–voltage (I – V) response of the PV device was measured in the dark and light under AM 1.5 solar illumination before electrochemical measurements. The open circuit voltage and short circuit current of the device were 423 mV and 19.3 mA cm^{-2} , respectively. The device was then electrochemically doped with Li^+ as described above. Fig. 4 shows I – V curves in the dark and under illumination after each doping experiment. The concentration of Li^+ in the Si is expressed in terms of the total charge (coulombs) passed through the device during the electrochemical experiments. Very little change in the I – V characteristics was observed for the Li^+ concentrations investigated here. In fact, the PV device showed a small increase in the photocurrent and fill factor with increasing Li^+ concentration. This increase in performance may originate from the increase in the conductivity of the Si substrate with Li content, decrease in recombination velocity within the Si depletion region due to filling of vacancies by Li^+ , or improved surface passivation.

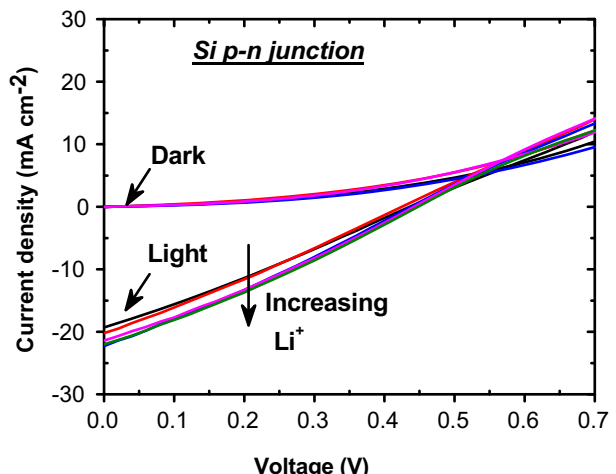


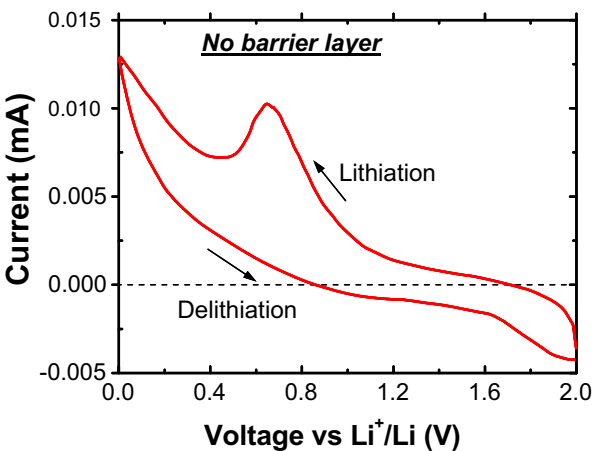
Fig. 4. I – V characteristics in dark and under 100 mW cm^{-2} AM 1.5 solar light of Si solar cell at increasing concentration of Li^+ . The total charge passed during the electrochemical insertion was $0, 0.03, 0.12, 0.43$, and 0.57 C cm^{-2} .

Thus, we conclude that the Si PV device is tolerant to Li^+ over the concentration range tested here.

Li^+ concentrations in the Si substrate higher than those tested here would lead to extensive amorphousization of the crystal structure and deterioration of PV device performance [13]. This can be avoided by placing a suitable barrier layer between the PV and battery so that a majority of Li^+ is prevented from diffusing into the substrate. This barrier layer would protect the PV component from unwanted physical damage and maintain a high battery capacity by preventing Li^+ loss from the active battery anode. Several materials including Ti, W, and TiN were investigated as potential barrier materials. Of these, TiN was found to be the most effective. In addition, TiN has good electrical conductivity. To test the efficacy of the barrier layer, a 50 nm Ti/200 nm W layer was first deposited on the n-doped side of the PV device by RF sputtering. The newly formed W/Ti/Si stack was annealed at 450 °C for 1 h to create an ohmic contact. On a separate sample, a 70 nm thick TiN film was deposited by RF sputtering to create a TiN/W/Ti/Si stack. Finally, 5 nm of Au catalyst was deposited on top of each sample (one with and the one without the final TiN layer) for Si nanowire growth. Si nanowires were grown directly on stainless steel for reference. Fig. 5 shows an SEM image of nanowires grown on top of the W/Ti/Si stack. No difference in nanowire morphology was observed for Si nanowires grown on W, TiN, or stainless steel. The samples are covered with randomly coiled nanowires, 80–100 nm diameter and several hundred μm in length.

Coulombic efficiencies for the battery were estimated from the electrochemical measurements. They were used as an indicator of the barrier layer's effectiveness at preventing Li^+ incorporation into the PV device. Si nanowires were used as the working electrode and Li foil was used as the counter and reference electrodes for the battery measurements. Contact to the working electrode was made through the W contact on the backside of the Si substrate, as shown in Fig. 6. The cyclic voltammogram in Fig. 6A shows a well-defined current peak corresponding to lithiation of the Si nanowire electrode on the W/Ti/Si stack with no TiN layer. There is little delithiation in this case because Li^+ are lost to the Si substrate and recovery would take an exceedingly long time, similar to Fig. 2. These data show that Ti and W alone cannot effectively block Li diffusion. Lithiation and delithiation experiments with a TiN barrier inserted between the Si nanowires and the W/Ti/Si stack are shown in Fig. 6B. Samples were cycled in the same way as that described above in the absence of the TiN barrier. Well-defined lithiation and delithiation peaks were observed because the Li was localized to

A



B

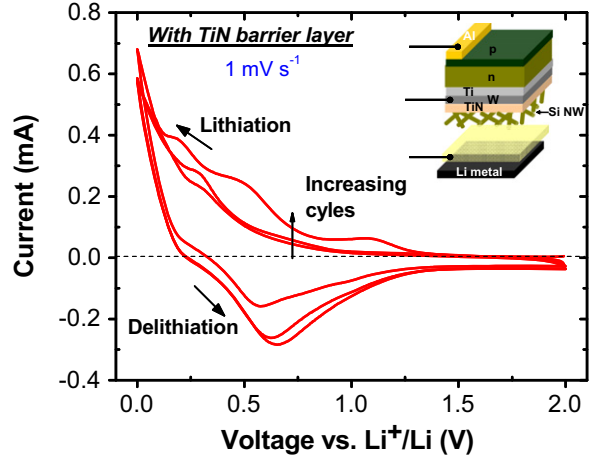


Fig. 6. Cyclic voltammogram of Si nanowires grown on top of the W/Ti/Si stack (A) with no barrier layer, (B) with TiN barrier layer during Li^+ intercalation and deintercalation at a scan rate of 1 mV s^{-1} .

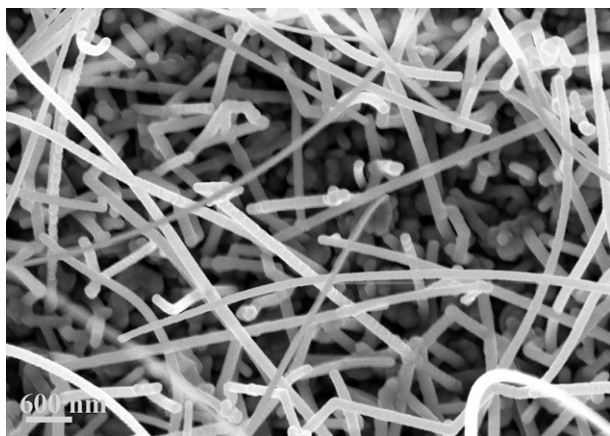


Fig. 5. SEM image of the Si nanowires grown on top of W/Ti/Si by the VLS technique for use as the battery anode. The nanowires had a diameter in the range of 80–100 nm and length of several hundred microns.

the Si nanowires and did not inset into the Si substrate. It should be noted that the as-deposited TiN is highly conducting and does not add a meaningful electrical resistance to the stack. The first charge (lithiation) and discharge (delithiation) capacities were 318.5 mC and 95.6 mC, respectively, corresponding to a Coulombic efficiency of 30%. The low Coulombic efficiency for the first cycle is partially due to SEI formation. Si nanowires grown on a stainless steel substrate showed a first cycle efficiency of 86% (not shown) and a steady state efficiency of 98% for all subsequent cycles [7]. On further cycling, the performance of the Si nanowire/TiN contact improved with second and third cycle efficiencies of 67% and 78%, respectively. Although a majority of the Li^+ is blocked by the TiN layer, there is some loss compared to the stainless steel control. Thus, a thicker or denser layer of TiN is likely needed to further improve the barrier performance. It has been shown that TiN deposited by atomic layer deposition has superior blocking properties compared to RF sputtered samples [14]. This option could be explored in a future study.

It is important to note that an organic electrolyte containing EC:DMC was used in the present study; however, our recent work has shown that ionic liquid electrolytes are a viable alternative to organic electrolytes [11]. The higher viscosity and negligible vapor pressure of ionic liquid electrolytes, as compared to the volatile organic electrolyte, may aid in sealing the integrated, PV-

battery device. It is important to reiterate that all Si nanowire anode testing was accomplished with nominally undoped Si nanowires at a relatively low current density without the use of conductive agents and binders. Although the resistivity of the Si nanowire may be initially high, it decreases with lithiation. This change in Si nanowire conductivity could change the site of lithiation during the experiment. A fully optimized integrated device could consist of doped nanowires mixed together with additional conductive agents to minimize resistive losses at high discharge rates.

4. Conclusion

A novel integrated energy harvester and storage scheme for wireless devices consisting of a Si-based PV device combined with a Si nanowire-based Li ion battery has been proposed. Some of the fabrication challenges and cross-contamination issues have been investigated. The I – V characteristics of lithiated PV devices were found to be tolerant to Li^+ contamination. TiN was identified as a Li^+ diffusion barrier, exhibiting a blocking efficiency as high as 78% for RF sputtered films.

Acknowledgments

The authors would like to thank Dr. Klaus Franzreb at Arizona State University for the assistance with SIMS measurement and

Prof. Bernard Kippelen and Dr. Yinhua Zhou for the use of their solar simulator. This work was funded by the Semiconductor Research Corporation through the Interconnect Focus Center, one of six Focus Center Research Programs.

References

- [1] E. Caamaño-Martín, D. Masa-Bote, A. Gutiérrez, F. Monasterio-Huelin, J. Jiménez-Leube, M. Castillo-Cagigal, and J. Porro, in 24th European Photovoltaic Solar Energy Conference, September 21–25, Hamburg, Germany, 2009, p. 3149.
- [2] L.J. Lauhon, M.S. Gudiksen, C.M. Lieber, Phil. Trans. R Soc. A 362 (2004) 1247.
- [3] B. Tian, X. Zheng, T.J. Kempa, Y. Fang, N. Yu, G. Yu, J. Huang, C.M. Lieber, Nature 449 (2007) 885.
- [4] R. M. Swanson, in Proceedings of the 31st IEEE Photovoltaic Specialists Conference 2005, p. 889.
- [5] M.D. Kelzenberg, D.B. Turner-Evans, M.C. Putnam, S.W. Boettcher, R.M. Briggs, J.Y. Bae, N.S. Lewis, H.A. Atwater, Energy Environ. Sci. 4 (2011) 866.
- [6] C.K. Chan, H. Peng, G. Liu, K. McIlwrath, X.F. Zhang, R.A. Huggins, Y. Cui, Nat. Nanotechnol. 3 (2008) 31.
- [7] V. Chakrapani, F. Rusli, M.A. Filler, P.A. Kohl, J. Power Sources 205 (2012) 433.
- [8] K. Peng, J. Jie, W. Zhang, S.-T. Lee, Appl. Phys. Lett. 93 (2008) 033105.
- [9] C.K. Chan, R. Ruffo, S.S. Hong, R.A. Huggins, Y. Cui, J. Power Sources 189 (2009) 34.
- [10] R. Ruffo, S.S. Hong, C.K. Chan, R.A. Huggins, Y. Cui, J. Phys. Chem. C 113 (2009) 11390.
- [11] V. Chakrapani, F. Rusli, M.A. Filler, P.A. Kohl, J. Phys. Chem. C 115 (2011) 22048.
- [12] M. Green, E. Fielder, B. Scrosati, M. Wachtler, J.S. Moreno, Electrochem. Solid-State Lett. 6 (2003) A75.
- [13] U. Kasavajjula, C. Wang, A.J. Appleby, J. Power Sources 163 (2007) 1003.
- [14] H.C.M. Knoops, L. Baggetto, E. Langereis, M.C.M. van de Sanden, J.H. Klootwijk, F. Roozeboom, R.A.H. Niessen, P.H.L. Notten, W.M.M. Kessels, J. Electrochem. Soc. 155 (2008) G287.